

***In Vitro* and *In Vivo* Evaluation of *N*-[2-[4-(3-Cyanopyridin-2-yl)piperazin-1-yl]ethyl]-3-[<sup>11</sup>C]methoxybenzamide, a Positron Emission Tomography (PET) Radioligand for Dopamine D<sub>4</sub> Receptors, in Rodents**

by Marcello Leopoldo<sup>a)</sup>, Svetlana V. Selivanova<sup>b)</sup>, Adrienne Müller<sup>b)</sup>, Enza Lacivita<sup>a)</sup>, John A. Schetz<sup>c)</sup><sup>d)1)</sup>, and Simon M. Ametamey<sup>\*b)1)</sup>

<sup>a)</sup> Dipartimento di Farmacia – Scienze del Farmaco, Università degli Studi di Bari ‘A. Moro’, via Orabona, 4, IT-70125 Bari

<sup>b)</sup> Center for Radiopharmaceutical Sciences of ETH, PSI and USZ, Department of Chemistry and Applied Biosciences of ETH Zurich, CH-8093 Zurich  
(phone: +41-44-6337463; fax: +41-44-6331367; e-mail: simon.ametamey@pharma.ethz.ch)

<sup>c)</sup> Department of Pharmacology & Neuroscience, University of North Texas Health Science Center, 3500 Camp Bowie Blvd, Fort Worth, TX, 76107-2699, USA

<sup>d)</sup> Institute of Aging and Alzheimer’s Disease Research, University of North Texas Health Science Center, 3500 Camp Bowie Blvd, Fort Worth, TX, 76107-2699, USA

---

The D<sub>4</sub> dopamine receptor belongs to the D<sub>2</sub>-like family of dopamine receptors, and its exact regional distribution in the central nervous system is still a matter of considerable debate. The availability of a selective radioligand for the D<sub>4</sub> receptor with suitable properties for positron emission tomography (PET) would help resolve issues of D<sub>4</sub> receptor localization in the brain, and the presumed diurnal change of expressed protein in the eye and pineal gland. We report here on *in vitro* and *in vivo* characteristics of the high-affinity D<sub>4</sub> receptor-selective ligand *N*-[2-[4-(3-cyanopyridin-2-yl)piperazin-1-yl]ethyl]-3-[<sup>11</sup>C]methoxybenzamide ([<sup>11</sup>C]2) in rat. The results provide new insights on the *in vitro* properties that a brain PET dopamine D<sub>4</sub> radioligand should possess in order to have improved *in vivo* utility in rodents.

---

**Introduction.** – Dopamine is an important neurotransmitter regulating key brain activities associated with endocrine function, motor control, and attention, motivation, and reward states *via* its interactions with five subtypes of metabotropic G protein-coupled receptors (GPCRs) [1]. The D<sub>2</sub>-like receptor family consists of three receptor subtypes, D<sub>2</sub>, D<sub>3</sub>, and D<sub>4</sub>, each of which couples to G<sub>i/o</sub> proteins and has high affinity for butyrophenone and substituted benzamide class ligands [2]. Although over 20 years have passed since the D<sub>4</sub> receptor was first cloned, its precise functional involvement in different pathologies and its distribution in the brain are still unclear [3–7]. Northern blot, RT-PCR, and *in situ* hybridization analyses have revealed the presence of low levels of D<sub>4</sub> mRNA in the cerebral cortex, amygdala, hippocampus, and striatum [8–12], and high levels of D<sub>4</sub> mRNA in retina and pineal gland [8][13]. Immunocytochemistry studies demonstrated D<sub>4</sub> receptor protein expression patterns similar, in many respects, to transcriptional patterns reported by others: D<sub>4</sub> receptor protein appeared to be localized to GABAergic neurons in the cerebral cortex, hippocampus,

---

1) Co-senior authors.

substantia nigra pars reticulata, globus pallidus, and a subset of cortical pyramidal neurons [14–20]. However, the sensitivity and selectivity of antibodies against the D<sub>4</sub> receptor have been questioned [21]. Moreover, ligand autoradiography studies have provided mixed results with the most recent studies suggesting that there is little or no D<sub>4</sub> receptor located in brain tissue [7].

In general, the densities of D<sub>4</sub> receptor expressed in brain, as determined by autoradiography or radioligand binding of tissue homogenates, have been reported to be relatively low (less than *ca.* 30 fmoles/mg protein) [7][22–26], though higher densities (*ca.* 135 fmoles/mg protein) have been reported in the retina [27]. Several lines of evidence suggest that the D<sub>4</sub> receptors expressed in retinal photoreceptor cells play an important role in the regulation of adaptive ocular responses and the control of circadian rhythm [28–33]. Expression of the D<sub>4</sub> receptor gene in the retina follows a diurnal circadian rhythm [30], and retinal D<sub>4</sub> receptors mediate the synchronization of circadian clocks by regulating the expression of other retinal genes [33]. The entrainment of photoreceptor cells serves to realign the retinal circadian clock with the environmental cycle. Misalignment of circadian and environmental cycles may be the underlying cause of numerous sleep disorders, including those associated with age-related insomnia, *Parkinson's* and *Alzheimer's* diseases, depression and bipolar disorder, blindness, and shift-work or jet lag [34–36]. The ability to non-invasively monitor the dynamics of the D<sub>4</sub> receptor in the retina and other central nervous system (CNS) structures would facilitate studies of the role of dopaminergic control of circadian rhythms under normal and pathological conditions.

A number of attempts have been made to identify a D<sub>4</sub>-selective PET radioligand (for a recent review, see [37]), but to date none is suitable due to the difficulty in combining very high D<sub>4</sub>-receptor affinity with high selectivity over other receptors and adequate ratios of specific to non-specific binding, the latter being the most challenging given the suspected low densities of the D<sub>4</sub> receptor. In the earliest attempts, the D<sub>1</sub>/D<sub>4</sub> receptor antagonist [<sup>11</sup>C]SDZGLC756 (*Fig. 1*) [38] was employed to visualize the D<sub>4</sub> receptor in the primate brain, following pre-administration with specific D<sub>1</sub>, D<sub>2</sub>, D<sub>3</sub>, and D<sub>5</sub> receptor subtype antagonists to block these non-D<sub>4</sub> dopamine receptors. Though widespread distribution of D<sub>4</sub> receptor was observed utilizing this approach, it was not applicable to human studies. The arylpiperazine derivative [<sup>11</sup>C]PB-12 (*Fig. 1*) with an extremely high specific activity (1810 GBq/μmol) was used for a PET imaging study in monkey, but its high non-specific binding resulted in a high background, making it impossible to determine its specific binding to the D<sub>4</sub> receptor [39]. Low non-specific binding in autoradiography experiments has been observed for [<sup>18</sup>F]1 (*Fig. 1*), but it is an unlikely candidate for *in vivo* PET studies in brain because of its relatively low binding potential ( $B_{\max}/K_D$ , ratio of expected receptor density (9–30 fmole/mg [7][27]) to the binding affinity of the radioligand to the receptor ( $K_i = 15$  nM)) [40]; most PET radioligands have a binding potential in the range of 3–10 [41].

Recently, we reported on the rational design of a set of high-affinity D<sub>4</sub> receptor benzamide derivatives [42] engineered to have low off-target affinity, low non-specific binding, and lipophilicity within the optimal range (*c logP* range of 2.5–3.5) for brain penetration by passive diffusion [43–45]. The derivative [<sup>11</sup>C]2 (*Fig. 1*) was selected for PET imaging studies in monkey, because the corresponding nonisotopic version of

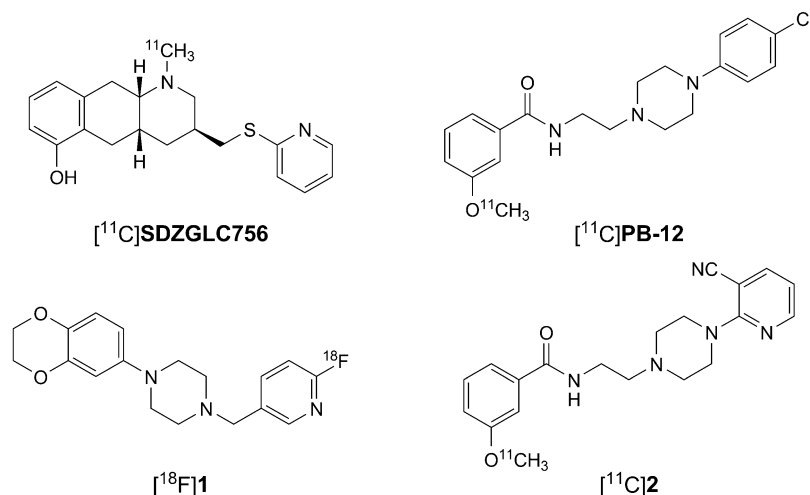
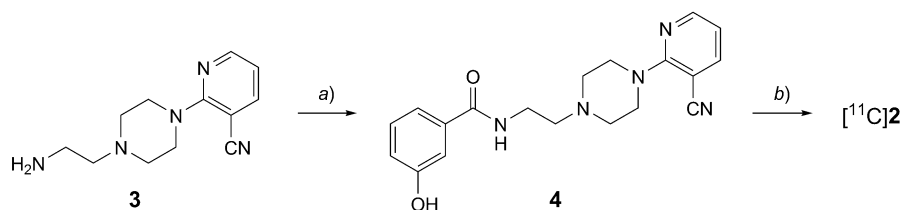


Fig. 1. Chemical structures of  $D_4$  dopamine receptor radioligands tested as PET imaging agents

this compound had high  $D_4$  receptor affinity ( $K_i = 1.52$  nM), lipophilicity suggestive of good brain penetration ( $\log P = 2.55$ ,  $\log D_{7.4} = 2.47$ ) and low non-specific binding, and excellent selectivity over a number of off-target receptors present in brain at higher densities than the predicted density of the  $D_4$  receptor ( $> 500$ -fold selectivity over dopamine  $D_2$  and  $D_3$  receptors, serotonergic 5-HT<sub>1A</sub>, 5-HT<sub>2A</sub>, and 5-HT<sub>2C</sub> receptors, and sigma<sub>1</sub> receptor [42]). Intense [<sup>11</sup>C]2 PET image signals in monkey were observed in the region of the posterior eye with little to no background signal in other parts of the brain including the cingulate, entorhinal, occipital, and cerebellar cortices, as well as the striatum and hippocampus [42]. However, even in a large primate, the resolution of the PET image was insufficient to determine localization within the microarchitecture of the eye. However, [<sup>11</sup>C]2 did have fast kinetics and a very low level of background binding, which are particularly useful features for imaging studies. Further, this ligand had only been investigated in primate and not in rodents, which are more amenable to detailed studies, in particular *ex vivo* studies. This prompted us to perform additional studies with [<sup>11</sup>C]2, in order to further explore the potential of [<sup>11</sup>C]2 to label specifically  $D_4$  receptors in the retina and in the CNS in rat.

**Results and Discussion.** – *Radiochemistry.* Phenol **4**, the demethyl precursor for <sup>11</sup>C-radiolabeling, was prepared as described by us (*Scheme*) in [42]. Briefly, 3-hydroxybenzoic acid was condensed with 4-(3-cyanopyridin-2-yl)-1-piperazinoethanamine (**3**) to give **4** in 40% yield. The identity was confirmed by <sup>1</sup>H-NMR spectroscopy and mass spectrometry. [<sup>11</sup>C]H<sub>3</sub>I was synthesized in a two-step reaction starting from the cyclotron derived [<sup>11</sup>C]O<sub>2</sub>. First, [<sup>11</sup>C]O<sub>2</sub> was catalytically reduced to [<sup>11</sup>C]H<sub>4</sub> followed by gas-phase free-radical iodination at elevated temperature resulting in [<sup>11</sup>C]H<sub>3</sub>I. Radiolabeling of the precursor **4** was achieved by reacting it with [<sup>11</sup>C]H<sub>3</sub>I to yield [<sup>11</sup>C]2. After HPLC purification and solvent removal, the compound was formulated in 0.9% saline for subsequent *in vitro* and *in vivo* evaluation. Radio-

Scheme



a) 3-Hydroxybenzoic acid, 1,1'-carbonyldiimidazole (CDI). b)  $[^{11}\text{C}]\text{H}_3\text{I}$ , NaOH.

chemical purity of the final product exceeded 99%. Specific radioactivity was in a range of 40–100 GBq/ $\mu\text{mol}$  at the end of synthesis ( $n=6$ ). The total synthesis time, including formulation, was 35–40 min from the end of bombardment. Radiochemical purity of the final product exceeded 99% as determined by analytical HPLC.

**Permeability Experiments.** For *in vivo* visualization of  $\text{D}_4$  receptors in the central nervous system (CNS), blood-brain barrier (BBB) permeability is a critical factor and can be estimated by permeability across Caco-2 cell monolayers [46]. Both physicochemical properties that promote passive diffusion (*e.g.*, lipophilicity, molecular weight, total polar surface area) and active efflux mechanisms, including P-glycoprotein (P-gp), are represented in this *in vitro* model of permeability. Therefore, we evaluated the efflux ratio (BA/AB) between basal-to-apical (BA) and apical-to-basal (AB) fluxes in Caco-2 cells monolayer of compound **2**. While the observed permeability ratio of 3.8 suggests that compound **2** is a substrate for P-gp, it is close to the cut-off value of 3 that is commonly used to distinguish P-gp substrates from nonsubstrates [47]. This result indicates that **2** is a relatively poor P-gp substrate and would thus be expected to accumulate in the CNS.

**In vitro Metabolic Stability.** The metabolic stability of compound **2** was estimated *in vitro* by incubating it with rat hepatic S9 fraction in the presence of an NADPH-generating system [48]. The S9 fraction contains both microsomes and cytosol, and it is thus representative of phase-I metabolism (cytochrome P450) and phase-II metabolism (transferases). After 30 min incubation in liver S9 fraction, LC/MS/MS analysis revealed a 70% loss of the parent compound. Analysis of the metabolites indicates compound **2** undergoes significant hydroxylation, but very little *O*-demethylation (Fig. 2). Because extraction conditions were optimized for maximal recovery of the parent compound **2**, we only gained insight for metabolites with physicochemical properties similar to those of the parent compound.

**Autoradiography Study.** *In vitro* autoradiography with  $[^{11}\text{C}]\mathbf{2}$  was performed on a cryosectioned *Wistar* rat brain and eye. The tissue slices were incubated with radiotracer solution of two different concentrations, 0.2 and 2 nM. Radiotracer binding was challenged by co-incubation with L-745,870 trihydrochloride, a high-affinity  $\text{D}_4$  dopamine receptor preferring antagonist ( $K_i=0.51$  nM) [49] with moderate affinity for  $\sigma_1$  receptors [50]. No binding to tissues was observed using a very low 0.2-nM concentration of  $[^{11}\text{C}]\mathbf{2}$  which would correspond to less than 15% receptor occupancy (Fig. 3). However, using 2 nM  $[^{11}\text{C}]\mathbf{2}$ , which would occupy over 55% of the receptors, significant binding was observed in the striatum (caudate and putamen) and around the

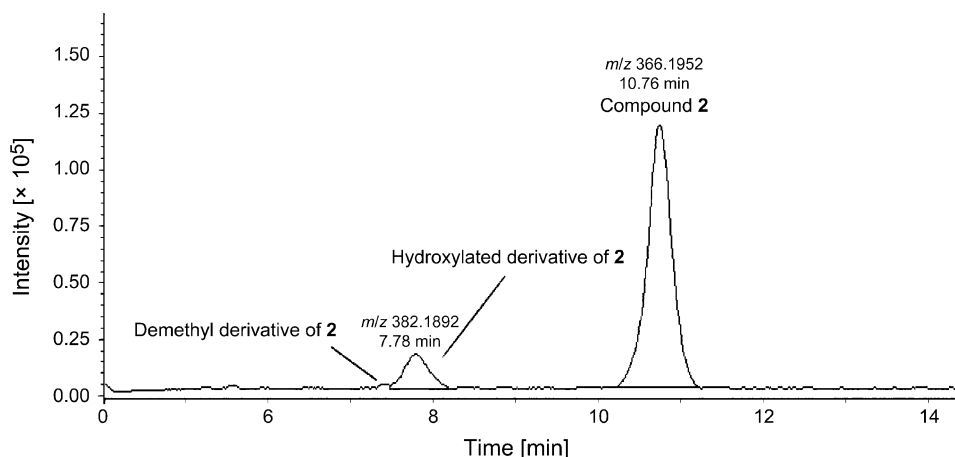


Fig. 2. LC/MS/MS Analysis of a sample of compound **2** after 30 min incubation with rat hepatic S9 fraction

circumference of the eye in the retinal region (Fig. 3). Binding of compound [ $^{11}\text{C}$ ]**2** to the retinal region of the eye was completely blocked with  $1\ \mu\text{M}$  L-745,870, demonstrating that it is specific for the  $\text{D}_4$  receptor, because this concentration of L-745,870 is sufficient to fully saturate  $\text{D}_4$  receptor ( $>99.9\%$  occupancy; Fig. 3). In contrast, the binding to the striatal region of the rat brain appears to be non-specific in nature, as it could only be partially blocked by  $1\ \mu\text{M}$  L-745,870 (Fig. 3).

**PET Study.** Rats were injected with *ca.* 40 MBq (0.6–1.0 nmol) of [ $^{11}\text{C}$ ]**2**, and their heads were subjected to PET scanning. In contrast to what was observed in monkey [42], no accumulation of [ $^{11}\text{C}$ ]**2** was clearly observable in rat in the posterior eye in the region of the retina (Fig. 4). Instead, high accumulation of radioactivity was visible in harderian and intraorbital lacrimal glands, which did not allow visualization of any accumulation in the eye due to a ‘spill over’ effect. Administration of the blocking compound, L-745,870, 30 min before injection of [ $^{11}\text{C}$ ]**2** did not diminish radioactivity uptake, indicating non-saturable, non-specific tracer accumulation in the glands.

**Conclusions.** – When exposed to cryosectioned tissue, the radioligand [ $^{11}\text{C}$ ]**2** specifically bound the  $\text{D}_4$  receptors in the rat eye in the region of the retina. Our autoradiography finding is consistent with the report on  $\text{D}_4$ -receptor protein in homogenates of rat retina detected with  $^{125}\text{I}$ -L-750,667, a differentially halogenated form of L-745,870 [27]. In our previous PET studies in monkey, [ $^{11}\text{C}$ ]**2** displayed a robust time-dependent accumulation in the posterior region of the eye, but very low, essentially undetectable accumulation was observed in the brain [42]. PET Studies of [ $^{11}\text{C}$ ]**2** in the eye of rats was not possible due to intense uptake of radiolabel in harderian glands, which potentially overshadowed any signal that might be observed in the rat retina, and highlights a species difference, as adult primates do not possess harderian glands [51]. In contrast, [ $^{11}\text{C}$ ]**2** autoradiography of rat brain sections revealed binding in the region of the striatum, that could not be displaced with a saturating concentration of the subnanomolar affinity  $\text{D}_4$ -receptor antagonist L-745,870, indicat-

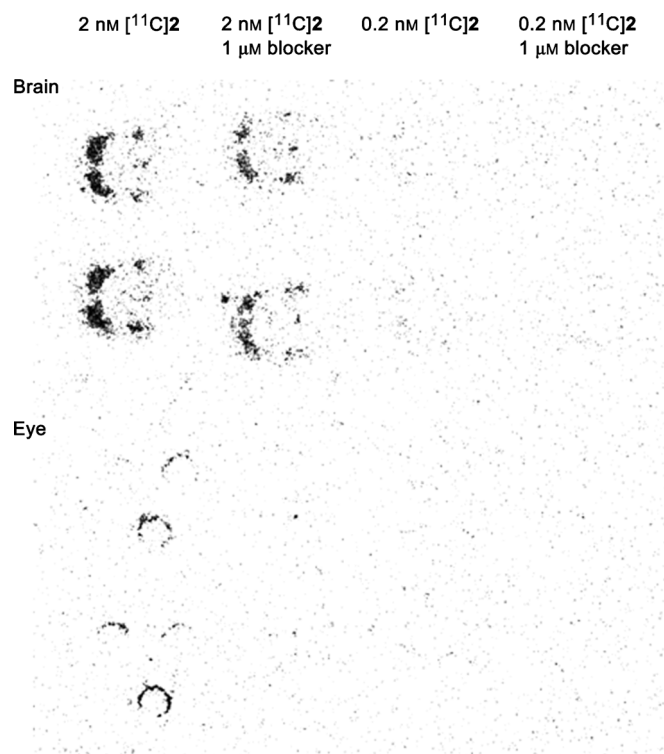


Fig. 3. Autoradiography study on coronal rat brain and eye sections using  $[^{11}\text{C}]\mathbf{2}$ . Binding of  $[^{11}\text{C}]\mathbf{2}$  to the rat eye was completely abolished in the presence of  $1\ \mu\text{M}$  L-745,870 trihydrochloride. Only partial blocking was observed in the rat brain.

ing that the binding of  $[^{11}\text{C}]\mathbf{2}$  to rat brain tissue was not due to specific interactions with the  $\text{D}_4$  receptor.

Radiotracers for imaging protein targets in the living brain with PET must fulfill many criteria, in terms of target affinity and selectivity, ability to cross the BBB, and pharmacokinetic properties. For each parameter, *in vitro* guideline values have been proposed over the years. Nonetheless, adherence to these guidelines does not allow *a priori* prediction of compound utility as a PET radioligand. The present study highlights the challenges of translating findings from *in vitro* models to *in vivo* applications, including interspecies differences. It is generally accepted that the  $B_{\text{max}}$  (concentration of the receptor protein) should exceed manyfold the  $K_d$  of the radioligand (ideally  $B_{\text{max}}/K_d > 10$ ). Since the  $B_{\text{max}}$  value for dopamine  $\text{D}_4$  in the brain is unknown but assumed to be very low, and the binding affinity of compound  $\mathbf{2}$  for the  $\text{D}_4$  receptor is  $K_i = 1.52\ \text{nM}$ , the next generation of  $\text{D}_4$  receptor PET radioligands should have subnanomolar affinity for the  $\text{D}_4$  receptor. However, increased affinity is often associated with increased lipophilicity for class A GPCRs, which tends to increase non-specific binding to lipid membranes, for example. While the low non-specific binding and good brain penetrance we observed in our previous study [42] seemed to indicate that compound

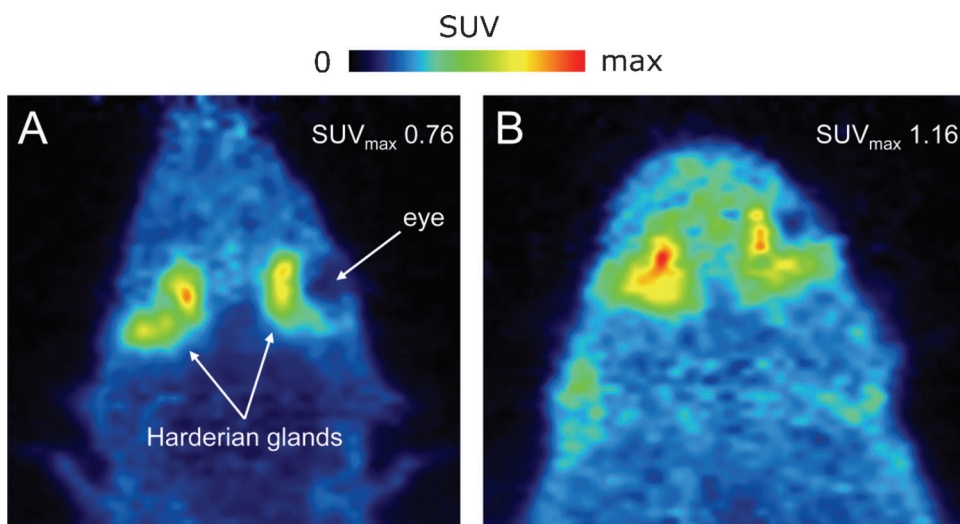


Fig. 4. PET Images (coronal slices) of the rat head after injection of  $[^{11}\text{C}]\mathbf{2}$  alone (A) or together with blocker, L-745,870 (B). PET Data were averaged from 0 to 20 min after tracer injection. High non-specific radioactivity uptake is observed in the harderian glands.

$\mathbf{2}$  has close-to-ideal lipophilicity properties for a PET ligand, this appears not to be the case in rodent if the target tissue is the eye, because rodents, but not primates, have harderian glands which apparently are depots for non-specific accumulation [52]. Besides the possibility of insufficient affinity of  $[^{11}\text{C}]\mathbf{2}$  for the target receptor, specific radioactivity of the radiotracer may have been inadequate, since the target receptor concentration is assumed to be very low. Thus, better metabolic stability of a radiotracer is also desired. When the eye is the target organ of interest, it is advisable to conduct PET studies in species that do not possess harderian glands to avoid misinterpretation of imaging results in cases where the radioligand accumulates in these glands. In summary, this study offers new insights on the *in vitro* properties that a brain PET dopamine  $\text{D}_4$  radioligand should possess to be successful *in vivo*.

#### Experimental Part

**Radiochemistry.**  $[^{11}\text{C}]\text{O}_2$  was produced via  $^{14}\text{N}(\text{p}, \alpha)^{11}\text{C}$  nuclear reaction by irradiation of  $\text{N}_2$  (containing 0.5%  $\text{O}_2$ ) gas target in a fixed energy Cyclone 18/9 cyclotron (IBA, Belgium).  $[^{11}\text{C}]\text{H}_3\text{I}$  was synthesized using an in-house-built automated unit starting from  $[^{11}\text{C}]\text{O}_2$  in a two-step reaction involving the catalytic reduction of  $[^{11}\text{C}]\text{O}_2$  to  $[^{11}\text{C}]\text{H}_4$  with a *Ra*-Ni catalyst and subsequent gas-phase free-radical iodination at  $720^\circ$  to  $[^{11}\text{C}]\text{H}_3\text{I}$  as described in [53].  $[^{11}\text{C}]\text{H}_3\text{I}$  was collected in a reaction vessel containing 300  $\mu\text{l}$  of anhydrous DMF solution of demethyl precursor  $\mathbf{4}$  (1 mg, 2.85  $\mu\text{mol}$ ) and NaOH (10  $\mu\text{l}$ , 0.5N) at r.t. After radioactivity in the reaction vessel reached a plateau, all the valves to the vessel were closed, and the mixture was heated at  $70^\circ$  for 3 min. The reaction was quenched with HPLC solvent (1.5 ml, MeCN/50 mM  $\text{HCOONH}_4$  45:55 buffer, pH 4.4) and injected into a semi-prep. HPLC for purification (column, reversed-phase (RP) Waters  $\mu\text{Bondapak C}_{18}$ ; particle size, 10  $\mu\text{m}$ , 125  $\text{\AA}$ , 300  $\times$  7.8 mm; mobile phase, MeCN/50 mM  $\text{HCOONH}_4$  45:55 buffer; pH 4.4; flow rate, 4 ml/min; detection, by UV at  $\lambda$  254 nm and with Eberline RM-14 radiodetector). The fraction at ca. 6 min corresponding to  $[^{11}\text{C}]\mathbf{2}$  was collected.

diluted with H<sub>2</sub>O (10 ml), and passed through a *C<sub>18</sub> Light SepPak* cartridge, preconditioned with EtOH (5 ml), followed by H<sub>2</sub>O (5 ml). The trapped radiotracer was washed with additional H<sub>2</sub>O and eluted with EtOH (1 ml) through a sterile filter into a sterile penicillin vial. The solvent was evaporated, and the residue was reconstituted in 0.9% saline (1 ml) for animal experiments. At the end of synthesis, 658–2930 MBq of [<sup>11</sup>C]2 was obtained as an injectable soln. The radiochemical purity and specific activity of [<sup>11</sup>C]2 were assayed by anal. HPLC using a *Agilent-Eclipse XDB-C<sub>18</sub>* column (particle size, 5 μm, 150 × 4.6 mm). The solvent system consisted of 50 mM HCOONH<sub>4</sub>/HCOOH (pH 4.4) as eluent *A* and MeCN as eluent *B* with a gradient as follows: 0–3 min, 10 to 50% *B*; 3–7 min, 50% *B* isocratic; 7–9 min, 50 to 70% *B*; and 9–10 min, 70% *B* isocratic; with a flow rate of 1 ml/min. Under these conditions [<sup>11</sup>C]2 was eluted at *t<sub>R</sub>* 4.87–4.98 min. For specific radioactivity determination, the area of the UV absorbance peak at 254 nm, corresponding to carrier product, was measured and compared to a standard calibration curve relating mass to UV absorbance. The identity of [<sup>11</sup>C]2 was confirmed by co-injection with an authentic non-radioactive sample.

**Preparation of Caco-2 Monolayer.** Caco-2 cells were seeded onto a *Millicell*<sup>®</sup> assay system (*Millipore*), where a cell monolayer is set in between a filter cell and a receiver plate, at a density of 10,000 cells/well. The culture medium was replaced every 48 h, and the cells were kept for 21 d in culture. The Trans Epithelial Electrical Resistance (TEER) of the monolayers was measured daily, before and after the experiment, using an epithelial volttohmmeter (*Millicell*<sup>®</sup>-ERS). Generally, TEER values > 1000 Ω for a 21-d culture are considered optimal.

**Drug Transport Experiment.** After 21 d of Caco-2 cell growth, the medium was removed from filter wells and from the receiver plate, which were filled with fresh HBSS buffer (*Hark's* balanced salt solution; *Invitrogen*). This procedure was repeated twice, and the plates were incubated at 37° for 30 min. After incubation time, the HBSS buffer was removed, and drug solns. and reference compound were added to the filter well at various concentrations (1–100 μM), while fresh HBSS was added to the receiver plate. The plates were incubated at 37° for 120 min. Then, samples were removed from the apical (filter well) and basolateral (receiver plate) side of the monolayer to measure the permeability.

The apparent permeability (*P<sub>app</sub>*), in nm/s, was calculated according the following equation:

$$P_{app} = \frac{V_A}{\text{area} \times \text{time}} \times \frac{[\text{drug}]_{\text{acceptor}}}{[\text{drug}]_{\text{initial}}}$$

where *V<sub>A</sub>* is the volume (in ml) in the acceptor well, area is the surface area of the membrane (0.11 cm<sup>2</sup> of the well), time is the total transport time in seconds (7200 sec), [*drug*]<sub>acceptor</sub> is the concentration of the drug measured by ESI-MS analyses or UV spectroscopy, and [*drug*]<sub>initial</sub> is the initial drug concentration (1 × 10<sup>-4</sup> M) in the apical or basolateral wells.

**Stability in Rat Liver S9 Fraction.** *In vitro* tests with rat liver S9 fraction (*BD Bioscience*, I-Milan) were designed as described by *Jia* and *Liu* with minor modifications [48]. Test compound (10 μM) was incubated with rat liver S9 fraction (1 mg/ml) in 100 mM phosphate buffer (pH 7.4) containing 1.3 mM of NADP<sup>+</sup>, 3.3 mM glucose 6-phosphate and 0.4 U/ml glucose 6-phosphate dehydrogenase, and 3.3 mM MgCl<sub>2</sub> in a total volume of 1 ml. Incubations were commenced with the addition of glucose 6-phosphate dehydrogenase and carried out for 30 min at 37°. The reaction was stopped by adding 1 ml of cooled MeCN. Immediately prior to adding MeCN, samples were spiked with an internal standard. The samples were centrifuged at 4,600 rpm for 15 min at 4°. The supernatant was separated, and the MeCN phase was analyzed by RP-HPLC. Samples from rat liver S9 incubation were analyzed by using a RP-HPLC equipped with a *PerkinElmer Series 200* LC pump and a *PerkinElmer 785A* UV/VIS detector. UV Signals were monitored, and obtained peaks were integrated using a PC running *PerkinElmer Turbochrom* Software. The column used was a *Phenomenex Gemini C<sub>18</sub>* (250 × 4.6 mm, 5 μm particle size). The sample was eluted with MeOH/H<sub>2</sub>O/Et<sub>3</sub>N 4:1:0.01 at a flow rate of 1 ml/min (λ 254 nm).

The percentage of the mean control concentration remaining after 30-min incubation was calculated according to the following equation:

$$\% \text{ of substrate remaining after 30 min} = C_{\text{parent}}/C_{\text{control}} \times 100$$

where  $C_{\text{parent}}$  is ligand concentration after incubation with S9 fraction and NADPH regenerating system, and  $C_{\text{control}}$  is ligand concentration after incubation with S9 fraction only. The main metabolites were identified by LC/MS/MS analysis with a *MicrOTOF-Q II* mass spectrometer (*Bruker Daltonics*); mass range, 50–800 *m/z*; electrospray ion source in positive-ion mode. Instrument settings: nebulizer gas,  $\text{N}_2$ , 2.5 bar; dry gas,  $\text{N}_2$ , 10 l/min; dry heater 200°; collision gas, Ar; cap. voltage, 4500 V; end plate offset voltage, –500 V; external calibration using cluster of  $\text{HCOONa}$ .

**Animals.** Male *Wistar* rats were obtained from Charles River (Germany). Animal care and all experimental procedures were approved by the Cantonal Veterinary Office in Zurich, Switzerland. The animals were allowed free access to food and water.

**In vitro Autoradiography.** Frozen coronal brain and eye cryosections (20  $\mu\text{m}$ ) from a male *Wistar* rat were thawed at ambient temp. and pre-incubated in *Tris* buffer (50 mM *Tris*·HCl, 120 mM NaCl, 1 mM EDTA, 5 mM  $\text{MgCl}_2$ , pH 7.4) for  $2 \times 5$  min. Excess pre-incubation soln. was removed, and slides were incubated with 0.2 nM or 2 nM [ $^{11}\text{C}$ ]2 alone or in the presence of 1  $\mu\text{M}$  or 10  $\mu\text{M}$  L-745,870 trihydrochloride in *Tris* buffer at r.t. for 30 min. The slides were washed in ice-cold *Tris* buffer for  $2 \times 5$  min, followed by brief dipping in ice-cold water. The air-dried slides were exposed to a phosphor imager plate (*BAS-TR 2025, Raytest-Fuji*) for 20 min, and the plate was visualized in a *BAS5000* reader (*Fujifilm*).

**In vivo PET Scans.** Rats (ca. 250 g) were immobilized by anesthesia with 2–3% isoflurane in  $\text{O}_2$ /air on a *GE Vista* explore PET/CT scanner (*Sedecal*) with the head in the field of view (axial field of view, 4.8 cm). Body temp. was controlled with a rectal probe connected to a 37° air blower, and respiratory frequency was monitored with a 1025T *Small Animal Monitoring and Gating System* (*SA Instruments*). At the start of data acquisition, 40.2 MBq, 0.5 nmol (baseline scan), and 38.5 MBq, 1 nmol (blocking experiment) of [ $^{11}\text{C}$ ]2 were injected into a tail vein, followed by 100  $\mu\text{l}$  of saline, and data were collected in list mode for 40 min. For the blocking, L-745,870 trihydrochloride (40 mg/kg, subcutaneous) was pre-injected 30 min before [ $^{11}\text{C}$ ]2 injection to block  $\text{D}_4$  binding sites and determine specific binding. A CT scan was performed for anatomical orientation following PET acquisition. PET Data were reconstructed with 2D-ordered subset expectation maximization (2D OSEM) algorithm and analyzed with PMOD 3.2 software (PMOD). Measured radioactivity values expressed as Bq/cm<sup>3</sup> were normalized to injected radioactivity per gram body weight (Bq/g) resulting in standardized uptake values (SUV).

## REFERENCES

- [1] J. M. Beaulieu, R. R. Gainetdinov, *Pharmacol. Rev.* **2011**, *63*, 182.
- [2] C. Z. Floresca, J. A. Schetz, *J. Recept. Signal Transduct. Res.* **2004**, *24*, 207.
- [3] D. Noaín, M. E. Avale, C. Wedemeyer, D. Calvo, M. Peper, M. Rubinstein, *Eur. J. Neurosci.* **2006**, *24*, 2429.
- [4] J. N. Oak, J. Oldenhof, H. H. Van Tol, *Eur. J. Pharmacol.* **2000**, *405*, 303.
- [5] J. A. Schetz, D. Sibley, in 'Handbook of Contemporary Neuropharmacology', Eds. D. Sibley, I. Hanin, M. J. Kuhar, P. Skolnick, John Wiley & Sons, Inc, Hoboken, NJ, 2007, pp. 221–256.
- [6] J. A. Schetz, in 'Dopamine receptors: introduction' IUPHAR database, 2009, available from: <http://www.iuphar-db.org/DATABASE/FamilyIntroductionForward?familyID=20>.
- [7] D. Marazziti, S. Baroni, I. Masala, G. Giannaccini, L. Betti, L. Palego, M. Catena Dell'Osso, G. Consoli, M. Castagna, A. Lucacchini, *Neurochem. Int.* **2009**, *55*, 643.
- [8] M. Matsumatu, K. Hidaka, S. Tada, Y. Tasaki, T. Yamaguchi, *Mol. Brain Res.* **1995**, *29*, 157.
- [9] M. S. Lidow, F. Wang, Y. Cao, P. S. Goldman-Rakic, *Synapse* **1998**, *28*, 10.
- [10] J. H. Meador-Woodruff, D. K. Grandy, H. H. Van Tol, S. P. Damask, K. Y. Little, O. Civelli, S. J. Watson Jr., *Neuropsychopharmacology* **1994**, *10*, 239.
- [11] J. H. Meador-Woodruff, V. Haroutunian, P. Powchik, M. Davidson, K. L. Davis, S. J. Watson, *Arch. Gen. Psychiatry* **1997**, *54*, 1089.
- [12] H. H. M. Van Tol, J. R. Bunzow, H.-C. Guan, R. K. Sunahara, P. Seemann, H. B. Niznik, O. Civelli, *Nature* **1991**, *350*, 610.
- [13] S. González, D. Moreno-Delgado, E. Moreno, K. Pérez-Capote, R. Franco, J. Mallol, A. Cortés, V. Casadó, C. Lluís, J. Ortiz, S. Ferré, E. Canela, P. J. McCormick, *PLoS Biol.* **2012**, *10*, e1001347.

- [14] L. Mrzljak, C. Bergson, M. Pappy, R. Huff, R. Levenson, P. S. Goldman-Rakic, *Nature* **1996**, *381*, 245.
- [15] A. Rivera, B. Cuellar, F. J. Giron, D. K. Grandy, A. de la Calle, R. Moratalla, *J. Neurochem.* **2002**, *80*, 219.
- [16] C. Mauger, B. Sivan, M. Brockhaus, S. Fuchs, O. Civelli, F. Monsma Jr., *Eur. J. Neurosci.* **1998**, *10*, 529.
- [17] Z. U. Khan, A. Gutierrez, R. Martin, A. Penafiel, A. Rivera, A. De La Calle, *J. Comp. Neurol.* **1998**, *402*, 353.
- [18] M. C. Defagot, E. L. Malchiodi, M. J. Villar, M. C. Antonelli, *Brain Res. Mol. Brain Res.* **1997**, *45*, 1.
- [19] M. A. Ariano, J. Wang, K. L. Noblett, E. R. Larson, D. R. Sibley, *Brain Res.* **1997**, *752*, 26.
- [20] M. C. Defagot, M. C. Antonelli, *Neurochem. Res.* **1997**, *22*, 401.
- [21] P. Rondou, G. Haegeman, K. Van Craenenbroeck, *Cell. Mol. Life Sci.* **2010**, *67*, 1971.
- [22] P. Seeman, H. C. Guan, H. H. Van Tol, *Nature* **1993**, *365*, 441.
- [23] R. A. Lahti, R. C. Roberts, A. C. Tamminga, *Neuroreport* **1995**, *6*, 2502.
- [24] R. J. Primus, A. Thurkauf, J. Xu, E. Yevich, S. McInerney, K. Shaw, J. F. Tallman, D. W. Gallager, *J. Pharmacol. Exp. Ther.* **1997**, *282*, 1020.
- [25] R. A. Lahti, R. C. Roberts, E. V. Cochrane, R. J. Primus, D. W. Gallager, R. R. Conley, C. A. Tamminga, *Mol. Psychiatry* **1998**, *3*, 528.
- [26] R. De La Garza, B. K. Madras, *Synapse* **2000**, *37*, 232.
- [27] S. Patel, K. L. Chapman, D. Marston, P. H. Hutson, C. I. Ragan, *Neuropharmacology* **2003**, *44*, 1038.
- [28] A. I. Cohen, R. D. Todd, S. Harmon, K. L. O'Malley, *Proc. Natl. Acad. Sci. U.S.A.* **1992**, *89*, 12093.
- [29] I. Nir, J. M. Harrison, R. Haque, M. J. Low, D. K. Grandy, M. Rubinstein, P. M. Iuvone, *J. Neurosci.* **2002**, *22*, 2063.
- [30] L. Bai, S. Zimmer, O. Rickes, N. Rohleder, H. Holthues, L. Engel, R. Leube, R. Spessert, *Brain Res.* **2008**, *1203*, 89.
- [31] L. L. Klitten, M. F. Rath, S. L. Coon, J. S. Kim, D. C. Klein, M. Møller, *Exp. Eye Res.* **2008**, *87*, 471.
- [32] C. R. Jackson, S. S. Chaurasia, H. Zhou, R. Haque, D. R. Storm, P. M. Iuvone, *J. Neurochem.* **2009**, *109*, 148.
- [33] C. R. Jackson, S. S. Chaurasia, C. K. Hwang, P. M. Iuvone, *Eur. J. Neurosci.* **2011**, *34*, 57.
- [34] N. Zisapel, *CNS Drugs* **2001**, *15*, 311.
- [35] D. P. Cardinali, A. M. Furio, M. P. Reyes, L. I. Brusco, *Cancer Causes Control* **2006**, *17*, 601.
- [36] B. Knie, M. T. Mitra, K. Logishetty, K. R. Chaudhuri, *CNS Drugs* **2011**, *25*, 203.
- [37] A. Banerjee, O. Prante, *Curr. Med. Chem.* **2012**, *19*, 3957.
- [38] C. Boy, A. Klimke, M. Holschbach, H. Herzog, H. Mühlensiepen, E. R. Kops, F. Sonnenberg, W. Gaebel, G. Stöcklin, R. Markstein, H. W. Müller-Gärtner, *Synapse* **1998**, *30*, 341.
- [39] O. Langer, C. Halldin, Y. Chou, J. Sandell, C. Swahn, K. Nägren, R. Perrone, F. Berardi, M. Leopoldo, L. Farde, *Nucl. Med. Biol.* **2000**, *27*, 707.
- [40] F. Kügler, W. Sihver, J. Ermert, H. Hübner, P. Gmeiner, O. Prante, H. H. Coenen, *J. Med. Chem.* **2011**, *54*, 8343.
- [41] C. Halldin, B. Gulyás, O. Langer, L. Farde, *Q. J. Nucl. Med.* **2001**, *45*, 139.
- [42] E. Lacivita, P. De Giorgio, I. T. Lee, S. I. Rodeheaver, B. A. Weiss, C. Fracasso, S. Caccia, F. Berardi, R. Perrone, M. R. Zhang, J. Maeda, M. Higuchi, T. Suhara, J. A. Schetz, M. Leopoldo, *J. Med. Chem.* **2010**, *53*, 7344.
- [43] E. Hellinger, S. Veszelka, A. E. Tóth, F. Walter, A. Kittel, M. L. Bakk, K. Tihanyi, V. Háda, S. Nakagawa, T. D. Duy, M. Niwa, M. A. Deli, M. Vastag, *Eur. J. Pharm. Biopharm.* **2012**, *82*, 340.
- [44] R. N. Waterhouse, *Mol. Imaging Biol.* **2003**, *5*, 376.
- [45] V. W. Pike, *Trends Pharmacol. Sci.* **2009**, *30*, 431.
- [46] M. Laruelle, M. Slifstein, Y. Huang, *Mol. Imaging Biol.* **2003**, *5*, 363.
- [47] S. A. Hitchcock, *J. Med. Chem.* **2012**, *55*, 4877.
- [48] L. Jia, X. Liu, *Curr. Drug Metab.* **2007**, *8*, 822.
- [49] J. J. Kulagowski, H. B. Broughton, N. R. Curtis, I. M. Mawer, M. P. Ridgill, R. Baker, F. Emms, S. B. Freedman, R. Marwood, S. Patel, S. Patel, C. I. Ragan, P. D. Leeson, *J. Med. Chem.* **1996**, *39*, 1941.
- [50] I. T. Lee, S. Chen, J. A. Schetz, *Eur. J. Pharmacol.* **2008**, *578*, 123.

- [51] A. P. Payne, *J. Anat.* **1994**, *185*, 1.
- [52] Y. Kuge, K. Minematsu, Y. Hasegawa, T. Yamaguchi, H. Mori, H. Matsuura, N. Hashimoto, Y. Miyake, *J. Cereb. Blood Flow Metab.* **1997**, *17*, 116.
- [53] P. Larsen, J. Ulin, K. Dahlstrom, *J. Label. Compd. Radiopharm.* **1995**, *37*, 73.

*Received May 8, 2014*